DISPLACEMENT-LENGTH RELATIONSHIPS OF NORMAL FAULTS ON MARS: NEW OBSERVATIONS WITH MOLA AND HRSC. E. Hauber[1] , E. Charalambakis[1], K. Gwinner[1], M. Knapmeyer[1], and M. Grott[1], [1]Institute of Planetary Research, German Aerospace Center (DLR), Rutherfordstr. 2, 12489 Berlin, Germany (Ernst.Hauber@dlr.de).

Introduction: The geometric properties of planetary fault populations can provide useful information on fractured rock bodies [e.g., 1]. However, so far only few data sets of the relationships between fault length and displacement have been measured for extraterrestrial faults [2], partly due to the limited number of reliable topographic datasets.

Here we use MOLA altimetry data [3] and HRSC images and Digital Elevation Models (DEM) [4] to obtain one or more displacement values for a given (normal) fault. This method allows us not only to measure the maximum displacement, but also to analyze the displacement distribution along the trace of a single fault. We compare our results to previous measurements on Mars and on Earth, and discuss the implications for further interpretation.

Data and Methods: We selected a fault population on the western Ophir Planum plateau in the Valles Marineris (VM) region for our preliminary analysis. This is an unnamed set of relatively complex, Late Hesperian-aged grabens between eastern Candor Chasma in the north and Coprates Chasma in the south (Fig. 1) [5]. It has characteristics that make it particularly useful for measurements with MOLA data: It has a fault trend which runs approximately WNW-ESE, which is ± perpendicular to single topographic MOLA profiles. This is important, since we measure fault offsets only at the location of MOLA tracks to avoid interpolation effects and to make use of the highest possible MOLA resolution. Another advantage is that the faults are relatively isolated, i.e. they do not cut major older fractures, and in turn are not cut and modified by younger fault populations (both would make the measurements much more complicated). We plot the single MOLA profiles on high-resolution HRSC images (12-20 m/pixel; mosaicked with a resolution of 50 m/pixel), and identify fault traces on the images. Fault lengths are measured in the images, and offsets across faults are measured in MOLA profiles (due to the distance between single MOLA tracks in E-W direction of typically a few km at the equator, we can obtain several offset measurements for a single fault only if the fault length is more than a few km; Fig. 2). With this information we can plot the displacement distribution on single faults (Fig. 5) as well as the displacement-length (D/L) relationship (Fig. 6). We present our preliminary assessments of displacement distributions (Fig. 5) assuming vertical fault planes. Usually, however, fault planes dipping 60° are assumed for Mars [e.g., 6], and even shallower dips for normal fault planes have been found [7]. Therefore, we apply a correction for 60°-dipping faults in the D/L plot (Fig. 6) for better comparison to other data sets [2].

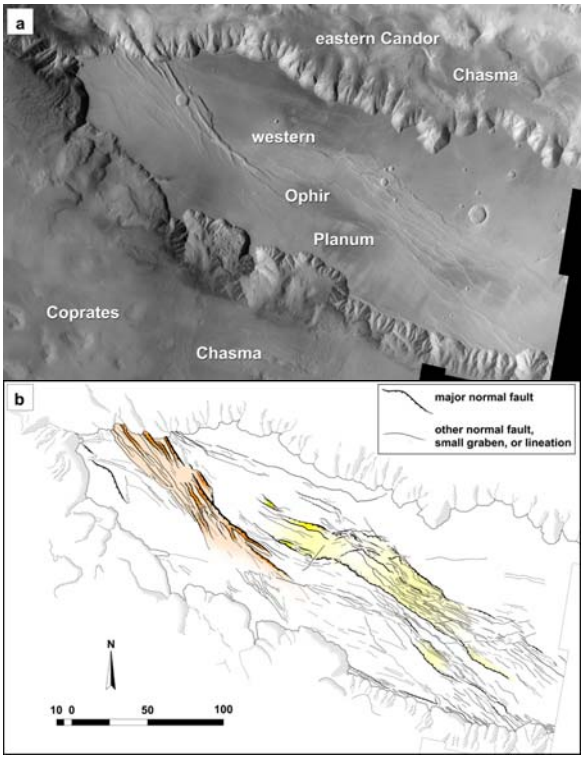

Fig. 1. Study area in Ophir Planum, centered at ~9.6°S and ~292.5°E. (a) Viking Orbiter image mosaic with physiographic features labeled. (b) Tectonic sketch map. The *en echelon* configuration of the two main fault sets (see [5]) is indicated by different color shading. We measured 145 faults in the "yellow" fault set.

Results: We measured the length of 1102 faults on Ophir Planum (fault array marked in yellow in Fig. 1b). For a subset of 145 faults, we additionally measured the topographic offset across the fault at several locations along the fault trace (Fig. 2) in single MOLA tracks. The displacement distribution of 12 faults has been measured in a high-resolution DEM derived from HRSC image data taken on Mars Express orbit 2039.

Fault length distribution. The cumulative frequency-length diagram (Fig. 3) exhibits a typical tri-segment shape [8]. The main branch can be approxi-

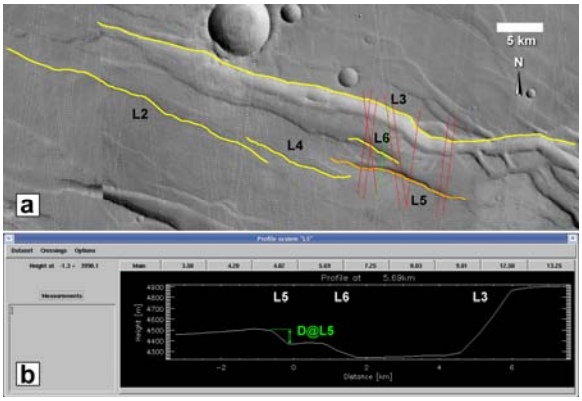

Fig. 2. Measurement technique. (a) HRSC image mosaic (50 m/pixel) and location of MOLA tracks (white dotted lines). Selected faults are marked with yellow lines and labeled (e.g., "L2"). Fault "L5" is selected (orange), and cross-sections used for offset measurements are marked in red. The active cross-section (see Fig 2b) is marked in green. (b) Screenshot of measurement window.

mated by a power law with a slope of about -2. The flattening ("roll-over") at shorter faults is ascribed to resolution effects, and the steepening at longer faults could be either a windowing effect, a systematic effect of low-topology sampling [9], or the result of post-faulting geologic processes like impact cratering that obscure the true length of long faults [10].

The shape of the curve displays a remarkable similarity to that obtained by [11] for independent (i.e., non-linked) faults in the VM area, but it is shifted toward shorter fault lengths. This shift might be ascribed

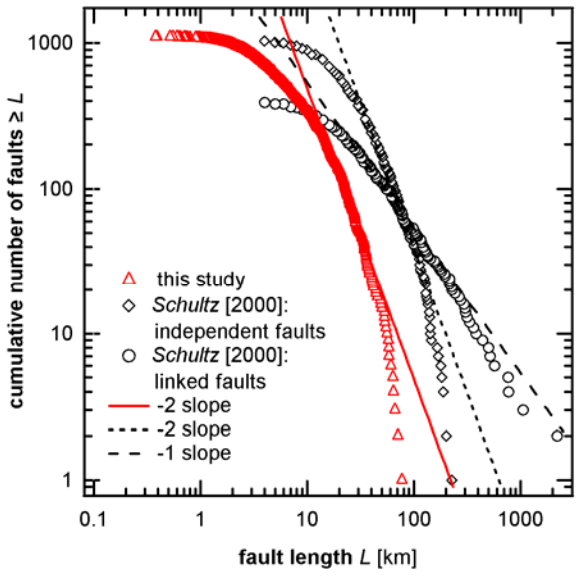

Fig. 3. Cumulative frequency-length diagram of "yellow" fault set (cf. Fig. 1b). Total number of faults is 1102. Black curves are from Table 1 in [9]. See text for details.

to the higher resolution of HRSC as compared to the Viking Orbiter images used by [11]. The similarity of the curves` shape might indicate that fault linkage in the Ophir Planum fault set is not a major mechanical process and that most of the measured faults are independent (note that the curve obtained by [11] for linked faults is different and follows a shallower slope). The relative steepness of the curve`s main branch might indicate that the fault population accommodated only small strain [12]. To test this possibility, we measured topographic offsets at all faults along a cross section perpendicular to the fault array. Using the method described in [13] and assuming 60° dipping of the fault planes, we obtained a cumulative extension of ~970 m, which corresponds to a strain of 2.1% (considering the width of the faulted zone only; strain would decrease if we had considered the total width of Ophir Planum). Compared to terrestrial continental rifts, this is a moderate amount of strain. We discuss the potential influence of fault linkage later.

Displacement Distribution along Faults. The displacement distribution along faults was measured from single MOLA tracks and from HRSC DEM. Gridded high-resolution HRSC DEM allow the measurement of profiles across a given fault at any position along the fault, leading toward a more reliable determination of D_{max}: If no MOLA tracks cross the area with the maximum displacement, D_{max} is underestimated in MOLA-based measurements (Fig. 4). The inspection of displacement distributions shows that both symmetric (position of D_{max} ~halfways between the fault tips) and asymmetric (D_{max} shifted toward one fault tip) patterns occur on Ophir Planum (Fig. 5). The shape of the distribution profiles is variable, and both triangular and

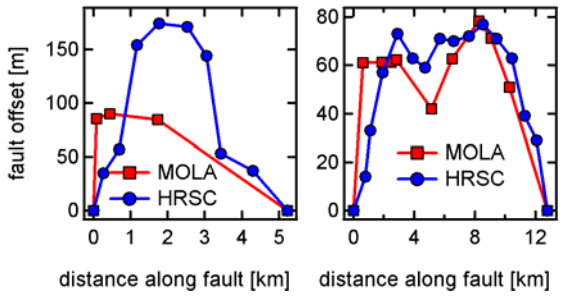

Fig. 4. Displacements at two faults, measured at single MOLA tracks and in HRSC DEM (the offset at the beginning and end of each fault was assumed to be zero). While the displacement profile is quite different for "short" faults (left), it is much more similar for "long" faults (right). This discrepancy results from the spacing between adjacent MOLA tracks, which can be several kilometers at low latitudes. Therefore, there is a high probability that MOLA-based measurements will yield smaller values for D_{max} (see also Fig. 5) where there is no MOLA fault at the location of D_{max}.

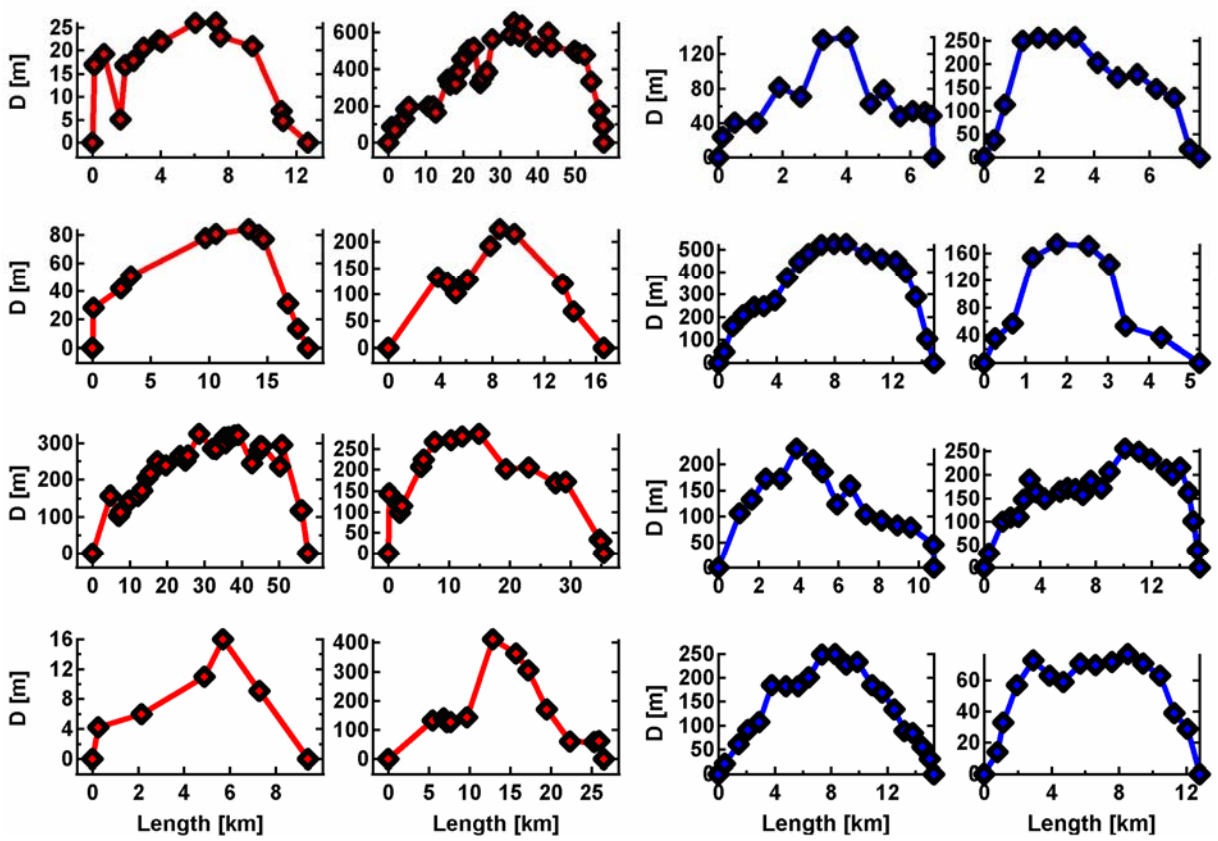

Fig. 5. Examples of observable displacement *D* along normal faults in Ophir Planum, assuming vertical fault planes. The topographic offsets were measured in single MOLA tracks (red) and HRSC DEM (blue). The offset at the beginning and end of each fault was assumed to be zero. Fault linkage is not considered, i.e. only isolated fault segments are shown. Note that due to the spacing between MOLA tracks it is possible to measure more profiles for shorter faults in HRSC DEM than in MOLA data (at least for mid- and low-latitude regions; see also Fig. 4).

semicircular-elliptic profiles can be observed.

Displacement-Length Relationship. The distribution D_{max} vs. fault length (L) shows a large scatter (Fig. 6). This phenomenon is often observed in terrestrial D-L plots, and can be ascribed to both geologic processes and measurement methods [14]. One possible explanation is fault growth by segment linkage, which leads to a step-like growth path of a fault in the D-L plot [15]. At first order, our results appear to be similar to previous measurements [6] from the northeastern branch of the Tempe Terra rift [13] (Fig. 6). However, a tendency for slightly higher displacements than those obtained by [6] can be observed. The most simple explanation would be that the relatively higher resolution of our data allowed for a more complete sampling of the offset distributions along a given fault, which resulted in the actual measurement of the maximum offset. Another factor leading toward relatively higher D_{max} values might be the fact that we measured separate fault segments only, since fault lengths increase in relation to the maximum offset if linkage is considered [9]. We expect that D/L values will shift towards lower D/L ratios if we consider fault linkage.

Fault Segmentation and Linkage. It is well known [e.g., 17] and has been demonstrated for the case of Mars [11] that fault linkage is an essential process in the growth of fault populations. In order to assess its influence on Ophir Planum, we constructed aggregate displacement profiles for en echelon faults. A preliminary visual inspection shows that linkage seems to be important in fault growth. Faults that are not connected via a well-developed relay ramp show an aggregate profile with two maxima (Fig. 7, fault array A). Where faults are connected via a breached relay ramp (Fig. 7, fault array B; Fig. 8), the aggregate profile approximates that of a fault with one maximum. This is typical for the throw distribution at linked faults [18].

Conclusion: (1) We developed a method for precise and efficient measurement of fault offsets from single MOLA tracks and high-resolution HRSC DEM. (2) We measured the lengths of >1,000 normal faults on Ophir Planum in the Valles Marineris region and

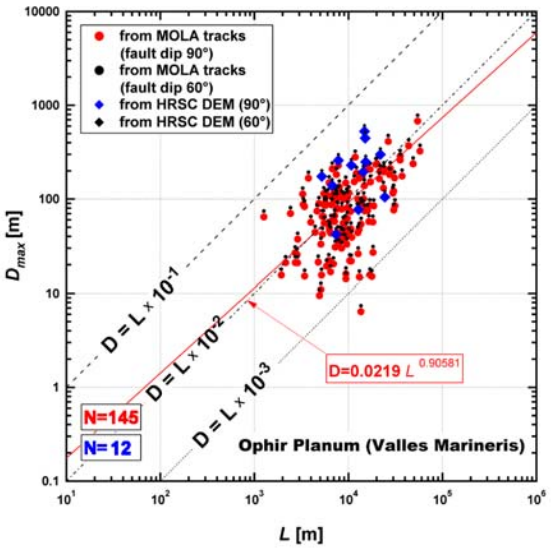

Fig. 6. D/L values for normal faults on Ophir Planum. Red dots mark topographic offsets as measured along single MOLA tracks, small black dots mark displacement on fault plane after correction for 60°-dipping fault planes (blue and small black diamond-shaped symbols: measurements from HRSC DEM for fault planes dipping 90° and 60°, respectively). The data show a relatively large scatter, but are comparable to data from terrestrial faults (D/L = ~1-5 × 10^{-2}; [2]; see also [16], where D_{max} = 0.03 * $L^{1.06}$).

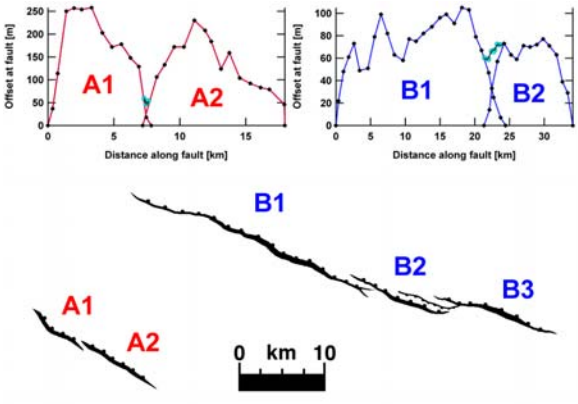

Fig. 7. (above) Aggregate distribution profiles across *en echelon* fault segments (symbols in cyan: sum of displacements). Left: Poorly linked faults; right: beginning fault linkage with breaching of relay ramp (stage 3 of [18]). (below) Tectonic sketch maps (N is up).

find that the shape of the size-frequency diagram can be approximated by a power-law with a slope of -2 for fault lengths between 10 km and 50 km. The steepness of the curve is in agreement with the small strain of 2%, determined from cumulative fault offsets and related to the width of the faulted zone. (3) Displacement-distance profiles along faults show variable shapes with both symmetric and asymmetric positions of D_{max}. Measurements in HRSC DEM tend to yield slightly larger D_{max} values due to the spacing between MOLA tracks at this low latitude-region. (4) HRSC DEM allow to measure displacement profiles for shorter faults than with MOLA data. (5) D/L ratios fall in the range of terrestrial normal faults [e.g., 16, 19] and are slightly higher than the results obtained by [6]. We will continue to measure faults in other areas on Mars like the Tempe Rift [13] and Acheron Fossae [20] and hope to close the gap between MOLA- [6] and HiRISE-based measurements [21].

References: [1] Schultz, R. A. (1999) *JSG*, *21*, 985-993. [2] Schultz, R. A. et al. (2006) *JSG*, *28*, 2182-2193. [3] Zuber, M. T. et al. (1992) *JGR*, *97*, 7781-7797. [4] Neukum, G. et al. (2004) *ESA SP-1240*, 17-35. [5] Schultz, R. A. (1989) *JGR*, *96*, 22,777-22,792. [6] Wilkins, S. J. et al. (2002) *GRL*, *29*, 1884, doi: 10.1029/2002GL015391. [7] Fueten, F. et al. (2007) *LPSC, XXXVIII*, abstract 1388. [8] Mansfield, C. and Cartwright (2001) *JSG*, *23*, 745-763. [9] Marrett, R. (1996) *JSG*, *18*, 169-178. [10] Schultz, R. A. and Fori, A. N. (1996) *JSG*, *18*, 373-383. [11] Schultz, R. A. (2000) *Tectonophysics*, *316*, 169-193. [12] Wojtal, S. F. (1996) *JSG*, *18*, 265-279. [13] Hauber, E. and Kronberg, P. (2001) *JGR*, *106*, 20,587-20,602. [14] Cowie, P. A. and Scholz, C. H. (1992) *JSG*, *14*, 1149-1156. [15] Cartwright, J. A. et al. (1995) *JSG*, *17*, 1319-1326. [16] Schlische, R. W. et al. (1996) *Geology*, *24*, 683-686. [17] Peacock, D. C. P. (2002) *Earth Sci. Rev.*, *58*, 121-142. [18] Peacock, D. C. P. and Sanderson, D. J. (1991) *JSG*, *14*, 721-733. [19] Scholz, C. H. (2002) *The Mechanics of Earthquakes and Faulting*, 2nd ed., Cambridge Univ. Press, 471 pages. [20] Kronberg, P. et al. (2007) *JGR, in press*. [21] Okubo, C. H. et al. (2007) *LPSC, XXXVIII*, abstract 1225.

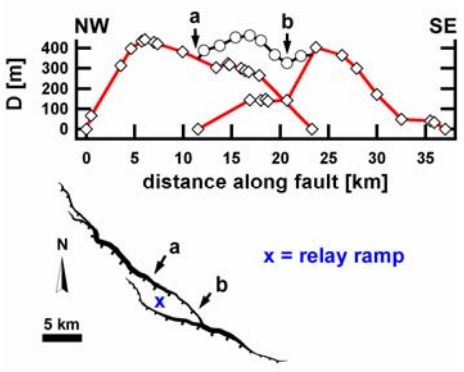

Fig. 8. Aggregate displacement profile for two en echelon faults connected by an almost completely breached relay ramp. The sum of the distribution profiles is shown by black line with circles. Displacement minima (a,b) can be observed where fault tips taper out.